Supporting Information

Nanoplasmonic core-shell nanoraspberry chip for ultrasensitive surface-enhanced Raman scattering detection of SARS-CoV-2: A modular nanobiosensor for respiratory virus diagnostics

Nnamdi Nwahara,[a] Saba Niaz,[a] Muthumuni Managa,[b] Christian I. Nkanga,[c] Oluwasesan Adegoke,[d] Ojodomo J. Achadu[a]

[a]School of Health and Life Sciences, and National Horizon Centre, Teesside University, Middlesbrough TS1 3BA, UK

[b]Institute for Nanotechnology and Water Sustainability (iNanoWS), Florida Campus, College of Science, Engineering and Technology, University of South Africa, Johannesburg 1710, South Africa.

[c]Centre de Recherche en Nanotechnologies Appliquées aux Produits Naturels (CReNAPN), Department of Medicinal Chemistry and Pharmacognosy, Faculty of Pharmaceutical Sciences, University of Kinshasa, B.P. 212, Kinshasa XI, Democratic Republic of the Congo.

[d]Leverhulme Research Centre for Forensic Science, School of Science & Engineering, University of Dundee, Dundee DD1 4GH, U.K

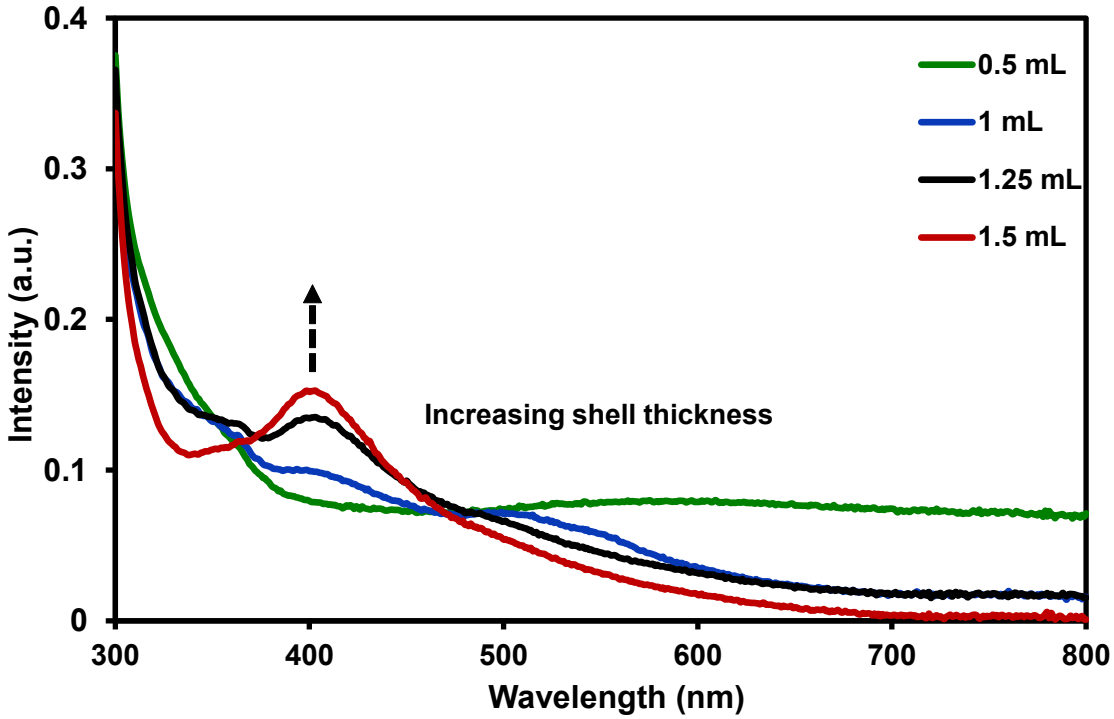

Fig. S1: Change in SPR with varying $AgNO_3$ volume added.

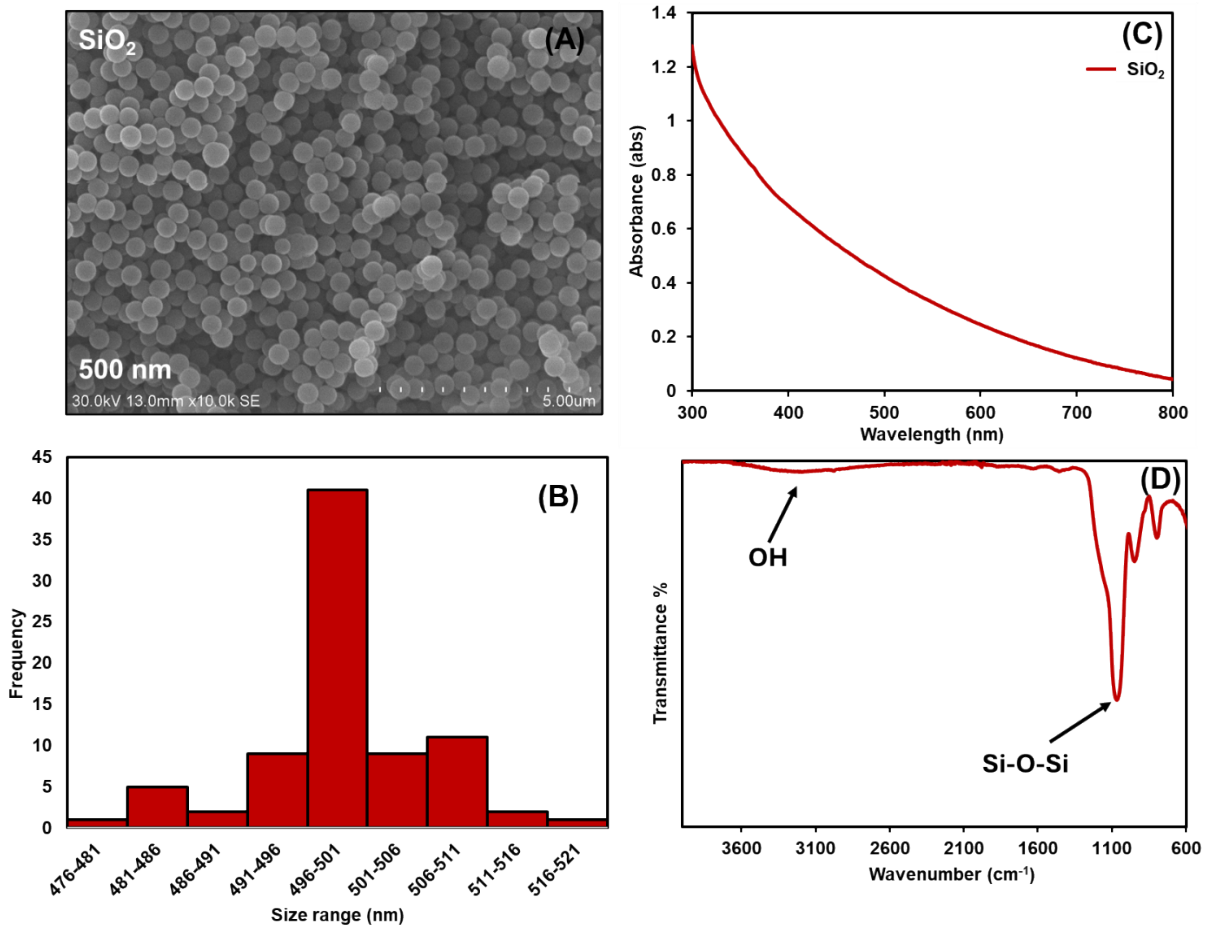

Fig. S2: (**A**) SEM image, (**B**) UV-Vis, (**C**) size distribution histogram, and (**D**) FTIR spectrum of as-synthesised SiO_2.

Fig. S3: XRD diffractograms of the bare FTO (black) and the Au-modified FTO-SiO_2-AuNPs surface.

Calculations of Enhancement Fator (EF):

The Raman scattering feature and subsequent SERS enhancement properties of the as-synthesized AuNRBs@ATP@Ag nanostructures were evaluated using the following equation (S1)[1]:

$$EF = \frac{I_S/N_S}{I_R/N_R}$$

Where, I_S, represents the integrated intensity of the SERS, I_R, is the normal Raman mode of the 4-ATP at the same peak. N_S, and N_R, are the numbers of the adsorbed 4-ATP molecules on the surface of the as-synthesized AuNRBs@ATP@Ag and the numbers of the ATP molecules alone excited at the engaged laser spot.

N_S (4.26 x 10^6) was calculated using the equation S2 below;

$$N_s = N_A \, x \, A/\sigma$$

Where, N_A, is Avogadro's constant, A is the effective area occupied by the Raman molecules under the laser irradiation , and σ is the per mol area of the molecules' monolayers (1.26 x 10^9 cm^2 mol^{-1})

The diameter of the laser spot was determined to be 1.1 μm using equation S3 below;

$$D = \left(\frac{\lambda}{NA}\right) x \, 1.22$$

Where, λ and NA are 785 nm and 0.9 as the Normal function, assuming a magnification of 100X, respectively. Start with diameter

LOD determination for SARS-CoV-2 S2 spike protein

For the calibration curve of the SERS assay shown in **Figure S4**, the limit of detection (LOD) for the SARS-CoV-2 S2 spike protein was determined using the slope (S) and y-intercept (c) of the calibration line, along with the standard deviations (σ) of the blank signal, as illustrated in **Fig. S4** below.

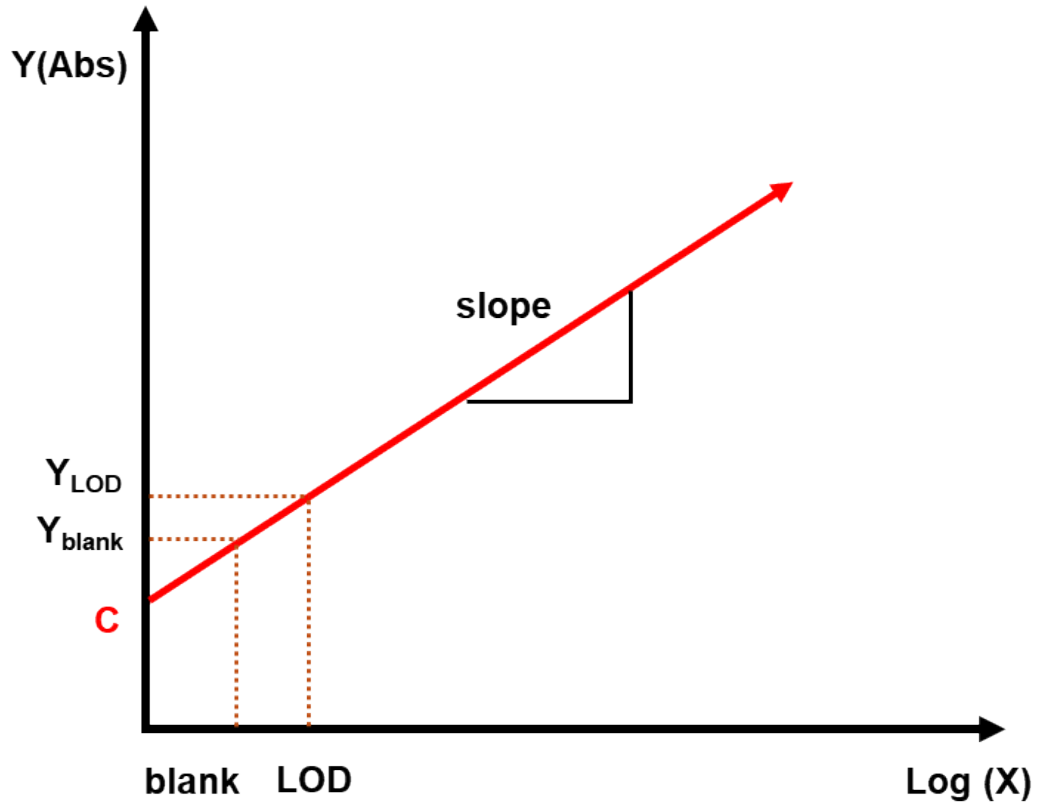

Fig. S4. Illustration of the LOD calculation for the SARS-CoV-2 S2 spike protein.

The calibration curve for the SERS intensity (Y) vs. spike protein concentration (X) is represented as a semi-log plot (Y, Ln X), the corresponding LODs were defined using (Khoris et al., 2021 [2]): [LOD] = $e^{3.3\sigma/S}$, according to the Eqs below.

$$Y = S \times Ln(X) + c \qquad \text{(S4)}$$

Where Y is the measured SERS intensity, X is the protein concentration (ng/mL), S is the slope of the calibration curve and c is the y-intercept.

The SERS signal corresponding to the LOD ($^{Y_{LOD}}$) is defined based on the blank signal and its standard deviation according to the equation below.

$$Y_{LOD} \leq Y_{blank} + 3.3 \times \sigma \qquad \text{(S5)}$$

Equating Eq. (S4) and Eq. (S5) gives:

$$S \times Ln(X_{LOD}) + c = Y_{blank} + 3.3 \times \sigma \qquad \text{(S6)}$$

The constant c is eliminated during the transition from Eq. (S6) to (S7) because the blank signal (Yblank) is equivalent to the y-intercept (c) of the calibration curve. When substituting Yblank = c into Eq. (S5) and equating it with the model in Eq. (S4), the c terms on both sides of the equation cancel out, leaving the LOD dependent solely on the sensitivity (slope, S) and the noise (standard deviation, σ).

Solving for X_{LOD}:

$$X_{LOD} = \exp\left(\frac{Y_{blank} + 3.3 \times \sigma}{S}\right) \qquad \text{(S7)}$$

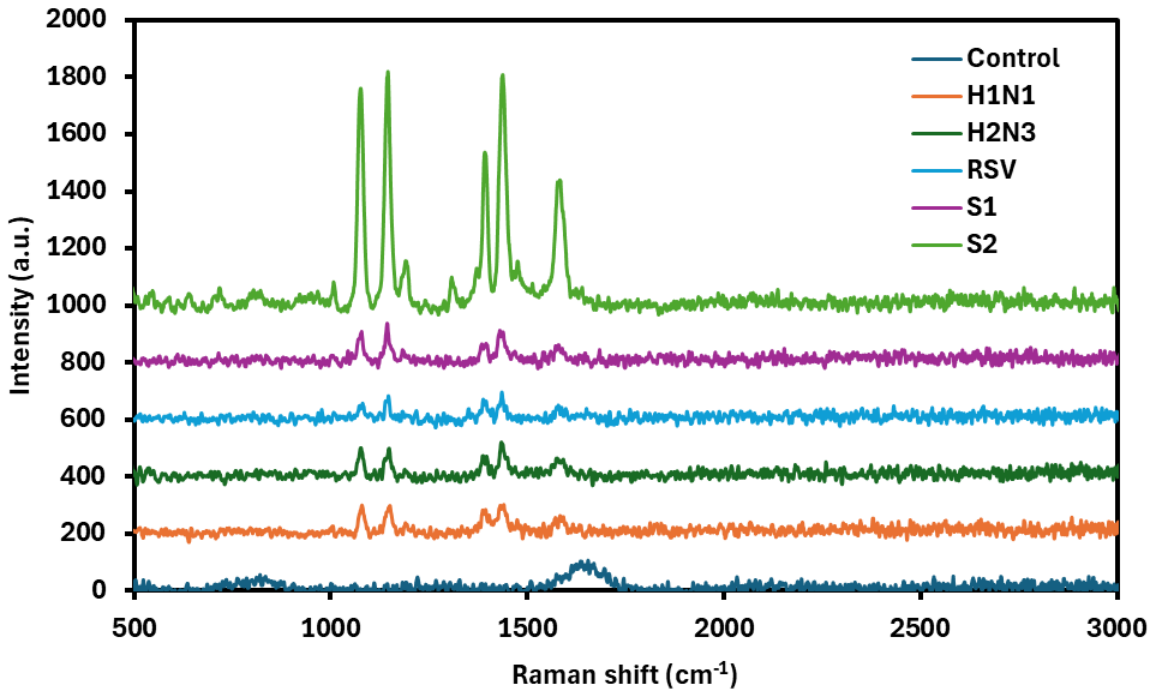

Fig. S5: SERS-based dual nanotag/sensor chip biosensing system for SARS-CoV-2. Representative Raman spectra for the specific detection of SARS-CoV-2 S2 in the presence of other viruses.

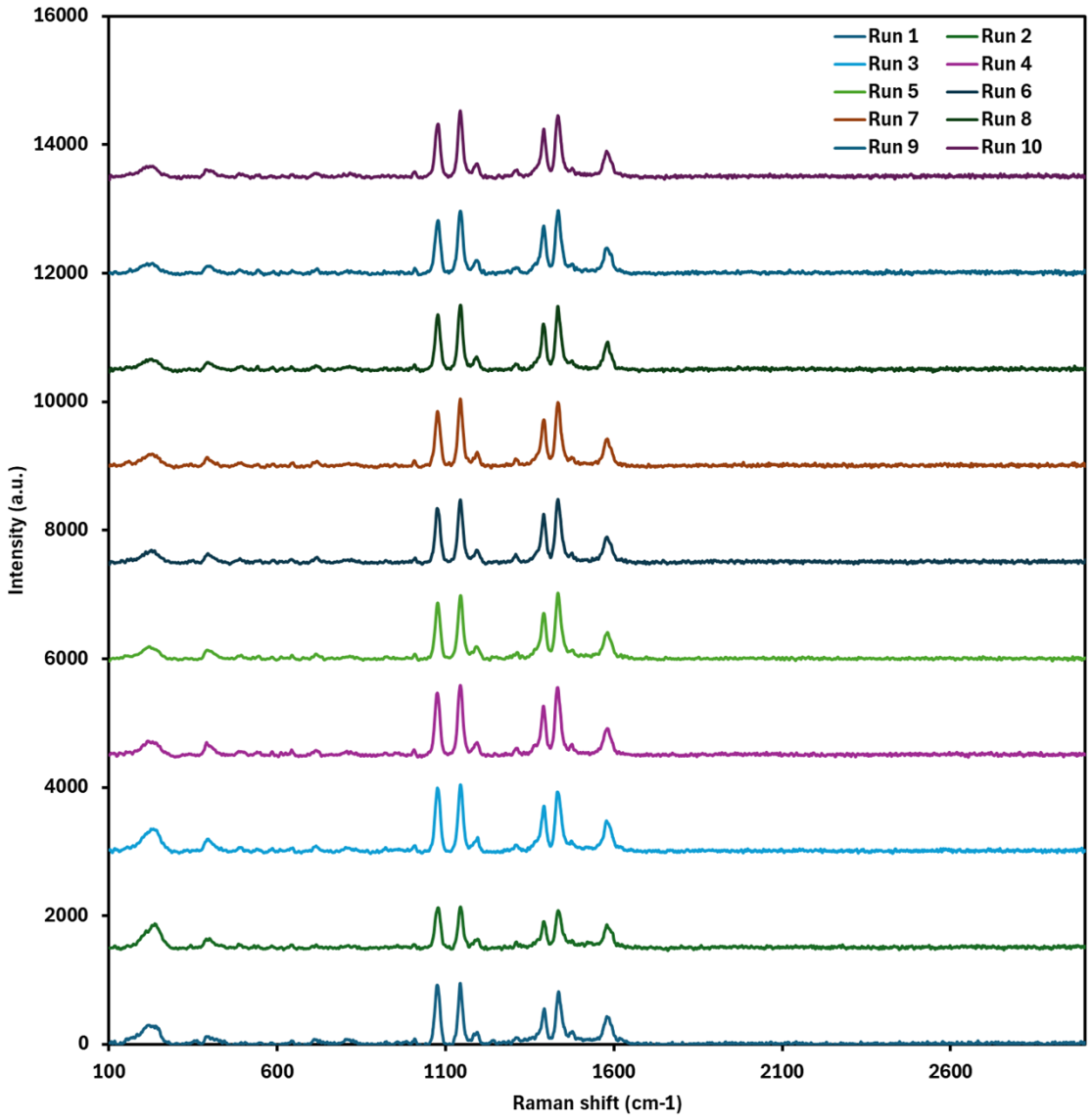

Fig. S6: SERS spectra of 4-ATP induced by 50 ng/mL of SARS-CoV-2 S2 collected at random spots on the sensor chip (n = 10).

Recovery analysis in Human Serum

The recovery value was obtained by back-calculating the concentration from the serum calibration equation $Y = aln(X) + b$. The calibration curve was constructed directly in spiked human serum; therefore, matrix effects were inherently accounted for. Using a log-linear fit on all measured points, the calibration equation is:

$$Y = 78.8\ln(X) - 26.9 \quad \text{(S7)}$$

(where S = 78.8 and c = -26.9)

Back-calculation recovery (single representative concentration)

Measured intensity at 2.5 ng/mL:

$Y = 42.187$

Back-calculate concentration:

$$X_{\text{calc}} = exp\left(\frac{Y - c}{S}\right) = exp\left(\frac{Y - 26.9}{78.8}\right)$$

$$X_{\text{calc}} = \exp(0.8768) = 2.4\ ng/mL$$

$$\text{Recovery (\%)} = \frac{2.4}{2.5} \times 100 = 96\ \%$$

Table S1: Analytical recovery of SARS-CoV-2 protein from spiked human serum samples.

Nominal concentration (ng mL⁻¹)	Measured SERS intensity (a.u.)	Back-calculated concentration (ng mL⁻¹)	Recovery %
2.5	42.19	2.4	96

References

[1] L. Zhou, J. Zhou, W. Lai, X. Yang, J. Meng, L. Su, C. Gu, T. Jiang, E.Y.B. Pun, L. Shao, L. Petti, X.W. Sun, Z. Jia, Q. Li, J. Han, P. Mormile, Irreversible accumulated SERS behavior of the molecule-linked silver and silver-doped titanium dioxide hybrid system, Nat. Commun. 11 (2020) 1785. https://doi.org/10.1038/s41467-020-15484-6.

[2] I.M. Khoris, K. Takemura, J. Lee, T. Hara, F. Abe, T. Suzuki, E.Y. Park, Enhanced colorimetric detection of norovirus using in-situ growth of Ag shell on Au NPs, Biosens. Bioelectron. 126 (2019) 425–432. https://doi.org/10.1016/j.bios.2018.10.067.